SCIENTIFIC REPORTS

OPEN

Controlling herding in minority game systems

Ji-Qiang Zhang[1], Zi-Gang Huang[1,2], Zhi-Xi Wu[1], Riqi Su[2] & Ying-Cheng Lai[2,3]

Received: 20 October 2015
Accepted: 13 January 2016
Published: 17 February 2016

Resource allocation takes place in various types of real-world complex systems such as urban traffic, social services institutions, economical and ecosystems. Mathematically, the dynamical process of resource allocation can be modeled as *minority games*. Spontaneous evolution of the resource allocation dynamics, however, often leads to a harmful herding behavior accompanied by strong fluctuations in which a large majority of agents crowd temporarily for a few resources, leaving many others unused. Developing effective control methods to suppress and eliminate herding is an important but open problem. Here we develop a pinning control method, that the fluctuations of the system consist of intrinsic and systematic components allows us to design a control scheme with separated control variables. A striking finding is the universal existence of an optimal pinning fraction to minimize the variance of the system, regardless of the pinning patterns and the network topology. We carry out a generally applicable theory to explain the emergence of optimal pinning and to predict the dependence of the optimal pinning fraction on the network topology. Our work represents a general framework to deal with the broader problem of controlling collective dynamics in complex systems with potential applications in social, economical and political systems.

Resource allocation is an essential process in many real-world systems such as ecosystems of various sizes, transportation systems (e.g., Internet, urban traffic grids, rail and flight networks), public service providers (e.g., marts, hospitals, and schools), and social and economic organizations (e.g., banks and financial markets). The underlying system that supports resource allocation often contains a large number of interacting components or agents on a hierarchy of scales, and there are multiple resources available for each agent. As a result, complex behaviors are expected to emerge ubiquitously in the dynamical evolution of resource allocation. In particular, in a typical situation, agents or individuals possess similar capabilities in information processing and decision making, and they share the common goal of pursuing as high payoffs as possible. The interactions among the agents and their desire to maximize payoffs in competing for limited resources can lead to vast complexity in the system dynamics.

Given resource-allocation system that exhibits complex dynamics, a defining virtue of optimal performance is that the available resources are exploited evenly or uniformly by all agents in the system. In contrast, an undesired or even catastrophic behavior is the emergence of herding, in which a vast majority of agents concentrate on a few resources, leaving many other resources idle or unused[1–12]. Herd behavior has also attracted much attention in traditional economics[13–16]. If this behavior is not controlled, the few focused resources would be depleted, possibly directing agents to a different but still small set of resources. From a systems point of view, this can lead to a cascading type of failures as resources are being depleted one after another, eventually resulting in a catastrophic breakdown of the system on a global scale. In this paper, we analyze and test an effective method to control herding dynamics in complex resource-allocation systems.

A universal paradigm to model and understand the interactions and dynamical evolutions in many real world systems is complex adaptive systems[17–19], among which minority game (MG)[20,21] stands out as a particularly pertinent framework for resource allocation. MG dynamics was introduced by Challet and Zhang to address the classic El Farol bar-attendance problem conceived by Arthur[22]. In an MG system, each agent makes choice (e.g., + or −, to attend a bar or to stay at home) based on available global information from the previous round of interaction. The agents who pick the minority resource are rewarded, and those belonging to the majority group are punished due to limited resources. The MG dynamics has been studied extensively in the past[21,23–40].

To analyze, understand, and exploit the MG dynamics, there are two theoretical approaches: mean field approximation and Boolean dynamics. The mean field approach was mainly developed by researchers from the

[1]Institute of Computational Physics and Complex Systems, Lanzhou University, Lanzhou Gansu 730000, China. [2]School of Electrical, Computer, and Energy Engineering, Arizona State University, Tempe, AZ 85287, USA. [3]Department of Physics, Arizona State University, Tempe, AZ 85287, USA. Correspondence and requests for materials should be addressed to Z.-G.H. (email: zghuang49@gmail.com)

statistical-physics community to cast the MG problem in the general framework of non-equilibrium phase transitions[21,20,41,42]. In the Boolean dynamics, for any agent, detailed information about the other agents that it interacts with is assumed to be available, and the agent responds accordingly[1–9,10–12]. Both approaches can lead to "better than random" performance in resource utilization. However, herding behavior in which many agents take identical action[43] can also take place, which has been extensively studied and recognized as one important factor contributing to the origin of complexity that leads to enhanced fluctuations and, consequently, to significant degradation in efficiency[1–12].

The control scheme we analyze in this paper is the pinning method that has been studied in controlling the collective dynamics, such as synchronization, in complex networks[11,44–50]. For the general setting of pinning control, the two key parameters are the "pinning fraction," the fraction of agents chosen to hold a fixed state, and the "pinning pattern," the configuration of plus or minus state assigned to the pinned agents. Our previous work[11] treated the special case of two resources of identical capacities, where the pinning pattern was such that the probabilities of agents pinned to positive or negative state (to be defined later) are equal. Note that, while the pinned agents are frozen during system's dynamical evolution, they are different from the "quenched" behavior in MG[23]. Especially, in our case the pinned states are a controlled state by design, but in typical MG dynamics the quenched behaviors are an emergent state through self organization. Here, we investigate a more realistic model setting and articulate a general mathematic control framework. A striking finding is that biased pinning control pattern can lead to an optimal pinning fraction for a variety of network topologies, so that the system efficiency can be improved remarkably. We develop a theoretical analysis based on the mean-field approximation to understand the non-monotonic behavior of the system efficiency about the optimal pinning fraction. We also study the dependence of the optimal fraction on the topological features of the system, such as the average degree and heterogeneity, and obtain a theoretical upper bound of the system efficiency. The theoretical predictions are validated with extensive numerical simulations. Our work represents a general framework to optimally control the collective dynamics in complex MG systems with potential applications in social, economical and political systems.

Results

Boolean dynamics. In the original Boolean system, a population of N agents compete for two alternative resources, denoted as $r=+$ and $r=-$, which have the same accommodating capacity $C_+ = C_- = N/2$. Similar to the MG dynamics, only the agents belonging to the *global minority* group are rewarded by one unit of payoff. As a result, the profit of the system is equal to the number of agents selecting the resource with attendance less than the accommodating capacity, which constitute the global-minority group. The dynamical variable of the Boolean system is denoted as A_t, the number of $+$ agents in the system at time step t. The variance of A_t about the capacity C_+ characterizes the efficiency of the system. The densities of the $+$ and $-$ agents in the whole system are $\rho_+ = A_t/N$ and $\rho_- = 1 - \rho_+$, respectively. The state of the system can be conveniently specified by the column vector $\hat{\rho} = (\rho_+, \rho_-)^{\mathrm{T}}$.

A Boolean system has two states (a binary state system), in which agents make decision according to the local information from immediate neighbors. The neighborhood of an agent is determined by the connecting structure of the underlying network. Each agent receives inputs from its neighboring agents and updates its state according to the Boolean function, a function that generates either $+$ and $-$ from the inputs[3]. Realistically, for any agent, global information about the minority choice from all other agents at the preceding time step may not be available. Under this circumstance, the agent attempts to decide the global minority choice based on neighbors' previous states. To be concrete, we assume[4,11] that agent i with k_i neighbors chooses $+$ at time step $t+1$ with the probability

$$P_{i\to\oplus} = \rho_-^i \equiv n_-^i(t)/[n_+^i(t) + n_-^i(t)], \tag{1}$$

and chooses $-$ with the probability $P_{i\to\ominus} = 1 - P_{i\to\oplus}$, where $n_+^i(t)$ and $n_-^i(t)$, respectively, are the numbers of $+$ and $-$ neighbors of i at time step t, with $k_i = n_+^i(t) + n_-^i(t)$. The expressions of probabilities, however, are valid only under the assumption that the two resources have the *same* accommodating capacity, i.e., $C_+ = C_-$. In real-world resource allocation systems, typically we have $C_+ \neq C_-$. Consider, for example, the extreme case of $C_+ \gg C_-$. Suppose we have $\rho_+^i = \rho_-^i$ for agent i. In this case, rationality demands a stronger preference to the resource $+$ (i.e., with a higher probability). To investigate the issues associated with the control of realistic Boolean dynamics, we define

$$\begin{pmatrix} P_{i\to\oplus} \\ P_{i\to\ominus} \end{pmatrix} = \mathbb{F}\cdot\hat{\rho}_i \equiv \begin{pmatrix} F_{+|+} & F_{+|-} \\ F_{-|+} & F_{-|-} \end{pmatrix}\cdot\begin{pmatrix} \rho_+^i \\ \rho_-^i \end{pmatrix}, \tag{2}$$

where $\mathbb{F}$ is the response function of each agent to its local environment $\hat{\rho}_i$, i.e., the local neighbor's configuration with $\rho_+^i = n_+^i(t)/k_i$ and $\rho_-^i = n_-^i(t)/k_i$. The quantity $F_{r|r'}$ (or $F_{r|r}$) characterizes the contribution of the r'-neighbors (or r-neighbors) to the probability for i to adopt r. The quantity $F_{r|r}$ represents the strength of *assimilation* effect among the neighbors, while $F_{r|r'}$ quantifies the *dissimilation* effect. Intuitively, the resource with a larger accommodating capacity would have a stronger assimilation effect among agents. By definition, the elements in each column in the matrix $\mathbb{F}$ satisfy $F_{r|r'} + F_{r'|r'} = 1$, i.e., the total probability for an agent to choose $+$ and $-$ is unity.

Using the mean-field assumption that the configuration of neighbors is uniform over the whole system, i.e., $\rho_+^i = \rho_+$, we have that the stable solution for Eq. (2) satisfies $\hat{\rho} = \mathbb{F}\cdot\hat{\rho}$, which leads to the eigenstate of $\mathbb{F}$ as

$$\hat{\rho}^* = \begin{pmatrix} \rho_+^* \\ \rho_-^* \end{pmatrix} = \begin{pmatrix} \dfrac{F_{+|-}}{F_{+|-} + F_{-|+}} \\ \dfrac{F_{-|+}}{F_{+|-} + F_{-|+}} \end{pmatrix}. \tag{3}$$

The rational response ($\mathbb{F}$) of agents to nonidentical accommodation capacities of resources will lead to the equality $\rho_+^*/\rho_-^* = C_+/C_-$, i.e., the stable fraction of the agent densities in $+$ and $-$ is simply the ratio of the capacities. The elements of $\mathbb{F}$ can then be defined accordingly using this ratio and the condition $0 \le F_{r|r'} \le 1$, which characterizes a stronger preference to the resource with a larger capacity. For the specific case of identical-capacity resources, we have $F_{+|-} = F_{-|+}$, and the solution reduces to the result $\hat{\rho}^* = (0.5,0.5)^{\mathrm{T}}$ of the original Boolean dynamics[4,11]. The optimal solution for the resource allocation is $A^* = N\rho_+^*$.

A general measure of Boolean system's performance is the variance of A_t with respect to the *capacity* C_+:

$$\sigma^2 = \frac{1}{T}\sum_{t=1}^{T}(A(t) - C_+)^2, \tag{4}$$

which characterizes, over a time interval T, the statistical deviations from the optimal resource utilization[4]. A smaller value of σ^2 indicates that the resource allocation is more optimal. A general phenomenon associated with Boolean dynamics is that, as agents strive to join the minority group, an undesired herding behavior can emerge, as characterized by large oscillations in $A(t)$. Our goal is to understand, for the general setting of nonidentical resource capacities, the effect of pinning control on suppressing/eliminating the herding behavior.

Pinning control scheme. Following the general principle of pinning control of complex dynamical networks[11,44–50], we set out to control the herding behavior by "pinning" a few agents to freeze their states during the dynamical evolution so as to realize optimal resource allocation for the entire network. Let ρ_p be the fraction of agents to be pinned, so the fraction of unpinned (or free) nodes is $\rho_f = 1 - \rho_p$. The numbers of the two different types of agents, respectively, are $N_f = N \cdot \rho_f$ and $N_p = N \cdot \rho_p$. The free agents make choices according to local time-dependent information, for whom the inputs from the pinned agents are fixed.

The two basic quantities characterizing a pinning control scheme are the order of pinning (the way how certain agents are chosen to be pinned) and the pinning pattern[11]. We adopt the degree-preferential pinning (DPP) in which the agents are selected to be pinned according to their connectivity or degrees in the underlying network. In particular, agents of higher degrees are more likely to be pinned. This pinning method originated from the classic control method to mitigate the effects of intentional attacks in complex networks[51–53]. The selection of the pinning pattern can be characterized by the fractions η_+ and η_- of the pinned agents that select $r = +$ and $r = -$, respectively, where $\eta_+ + \eta_- = 1$. The quantities η_+ and η_- are thus the *pinning pattern indicators*. Different from the previous work[11] that investigated the specific case of $\eta_+ = \eta_- = 0.5$ (half-half pinning pattern), here we consider the more general case where η_+ is treated as a variable. The pinning schemes are implemented on random networks and scale-free networks with different values of the scaling exponent γ in the power-law degree distribution[54,55] $P(k) \sim k^{-\gamma}$. As we will see below, one uniform optimal pinning fraction ρ_p exists for various values of the pinning pattern indicator η_+.

Simulation Results. To gain insight, we first study the original Boolean dynamics with $C_+/C_- = 1$ and $\mathbb{F} = (0,1;\ 1,0)$ for different values of the pinning pattern indicator η_+. The game dynamics are implemented on scale-free networks of size $N = 1001$ and of the scaling exponent $\gamma = 3.0$[54] with the average degree $\langle k\rangle$ ranging from 6 to 40. The DPP scheme is performed with pinning fraction ρ_p and η_+ values ranging from 0.6 to 1.0 (i.e., all to $+$ pinning). The variance σ^2 versus ρ_p for different values of η_+ and different degree $\langle k\rangle$ are shown in Fig. 1. We see that, in general, systems with larger values of η_+ exhibit larger variance, implying that a larger deviation of η_+ from the ratio of the capacity C_+/N can lead to lower efficiency in resource allocation. Surprisingly, there exists a universal optimal pinning fraction (denoted by ρ_p^*) about 0.4, where the variance σ^2 is minimized and exhibits an opposite trend for $\rho_p > \rho_p^*$, i.e., larger values of η_+ result in smaller values of σ^2. The implication is that, deviations of η_+ from C_+/N provide an opportunity to achieve better performance (with smaller variances σ^2), due to the non-monotonic behavior of σ^2 with ρ_p. To understand the emergence of the optimal pinning fraction ρ_p^*, we see from Fig. 1 that the values of ρ_p^* are approximately identical for different values of η_+, which decrease with the average degree $\langle k\rangle$. As we will see below, in the large degree limit $k \to \infty$, the value of σ^2 can be predicted theoretically (c.f. Fig. 4).

Simulations using scale-free networks of different degrees of heterogeneity also indicate the existence of the universal optimal pinning control scheme, as can be seen from the behaviors of the variance calculated from scale-free networks of different degree exponents (Fig. 2)[55], where smaller values of γ point to a stronger degree of heterogeneity of the system. We see that an optimal value of ρ_p^* exists for all cases, which decreases only slightly with γ, i.e., more heterogeneous networks exhibit larger values of the optimal pinning fraction ρ_p^*, a phenomenon that can also be predicated theoretically (c.f. Fig. 5).

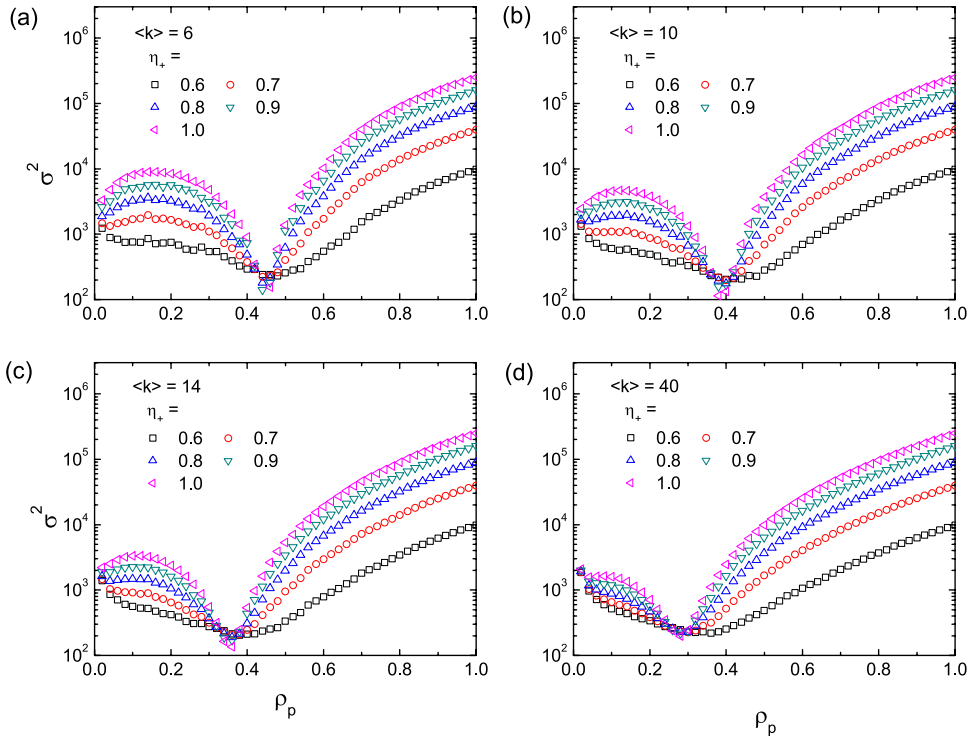

Figure 1. Variance σ^2 as a function of the pinning fraction ρ_p for scale-free networks of different connection densities. The average degree of the networks for simulation are $\langle k\rangle = 6$, 10, 14, to 40 in (**a–d**), respectively, and the value of the pinning pattern indicator η_+ ranges from 0.6 to 1.0 for each panel. The results are averaged over 200 realizations for scale-free networks of size $N = 1001$ and degree exponent $\gamma = 3.0$. In each realization, the system evolves for 10000 time steps, and σ^2 is calculated from the corresponding $A(t)$, with the first 3000 time steps discarded to avoid the influence of transient state.

Theoretical Analysis. The phenomenon of the existence of a universal optimal pinning fraction ρ_p^*, independent of the specific values of pinning pattern indicator η_+, is remarkable. Here we develop a quantitative theory to explain this phenomenon.

To begin, we note that MG is effectively a stochastic dynamical process due to the randomness in the selection of states by the agents. The variance of the system, a measure of the efficiency of the system, is determined by two separated factors. The first, denoted as $X_1(\delta)$, is the intrinsic fluctuations of A about its expected value A^*, defined as $\delta \equiv \sqrt{\langle (A - A^*)^2\rangle}$, which can be calculated once the stable distribution of attendance $P(A)$ is known, where $P(A)$ can be obtained either analytically (c.f., Fig. 3) or numerically. The second factor, denoted as $X_2(\varepsilon)$, is the difference of the expected value A^* from the capacity C_+ of the system: $\varepsilon \equiv A^* - C_+$, which also contributes to the variance of the system. Taking into account the two factors, we can write the system variance σ^2 [defined in Eq. (4)] as

$$\sigma^2 \equiv \langle (A - C_+)^2\rangle = \langle (A - A^* + A^* - C_+)^2\rangle = \delta^2 + \varepsilon^2, \tag{5}$$

which is a sum of two factors: $X_1(\delta) = \delta^2$ and $X_2(\varepsilon) = \varepsilon^2$. In contrast to the special case of $A^* = C_+$ treated in previous works[4,11], the more general cases are that the expected value A^* is not equal to the capacity C_+. Nonzero values of ε are a result of the biased pinning pattern ($\eta_+ \neq 0.5$) or improper response to the limited capacities of the resources. In fact, recent studies of the flux-fluctuation law in complex dynamical systems indicated that the variance of the system is determined by the two factors: intrinsic fluctuations and external driving[56–62].

Stable distribution of attendance. To quantify the process of biased pinning control, we derive a discrete-time master equation and then discuss the effect of network topology on control.

Discrete-time master equation for biased pinning control. To understand the response of the Boolean dynamics to pinning control with varied values of the pinning pattern indicator η_+, we generalize our previously developed analysis[11]. Let P_p be the probability for a *neighbor* of one given *free* agent to be pinned so that the probability of encountering a free agent is $P_f = 1 - P_p$. The transition probability of the system from $A(t)$ to $A(t+1)$ can be expressed in terms of η_+. In particular, note that the state transition is due to updating of the N_f free agents, as the remaining N_p agents are fixed. To simplify notations, we set $A(t) = i$, $A(t+1) = k$, and $A(t+2) = j$, for $i, k, j \in [0, N]$. The conditional transition probability from i at t to k at $t+1$ is

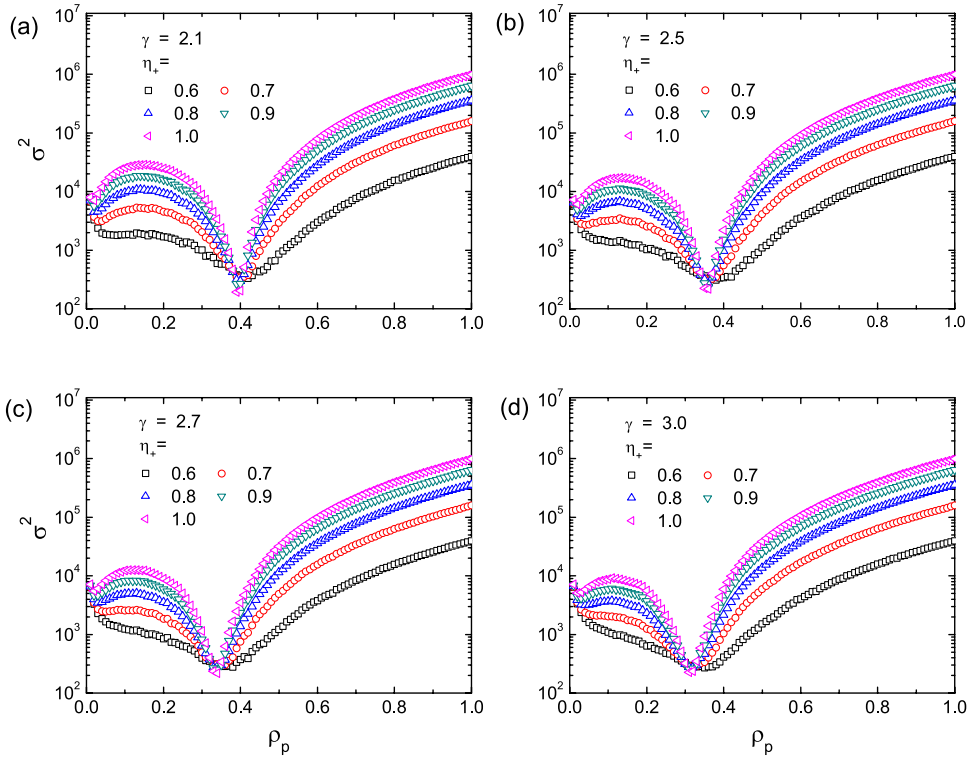

Figure 2. Variance σ^2 as a function of the pinning fraction ρ_p for scale-free networks of varying degrees of heterogeneity. The scaling exponents of the networks are $\gamma = 2.1$, 2.5, 2.7, and 3.0 in (**a**–**d**), respectively, and the value of the pinning pattern indicator η_+ ranges from 0.6 to 1.0 for each panel. The results are averaged over 200 realizations for scale-free networks of size $N = 2001$ and average degree $\langle k \rangle \approx 4$. In each realization, the system evolves for 10000 time steps, and σ^2 is calculated from the corresponding $A(t)$, with the first 3000 time steps discarded to avoid the influence of transient state.

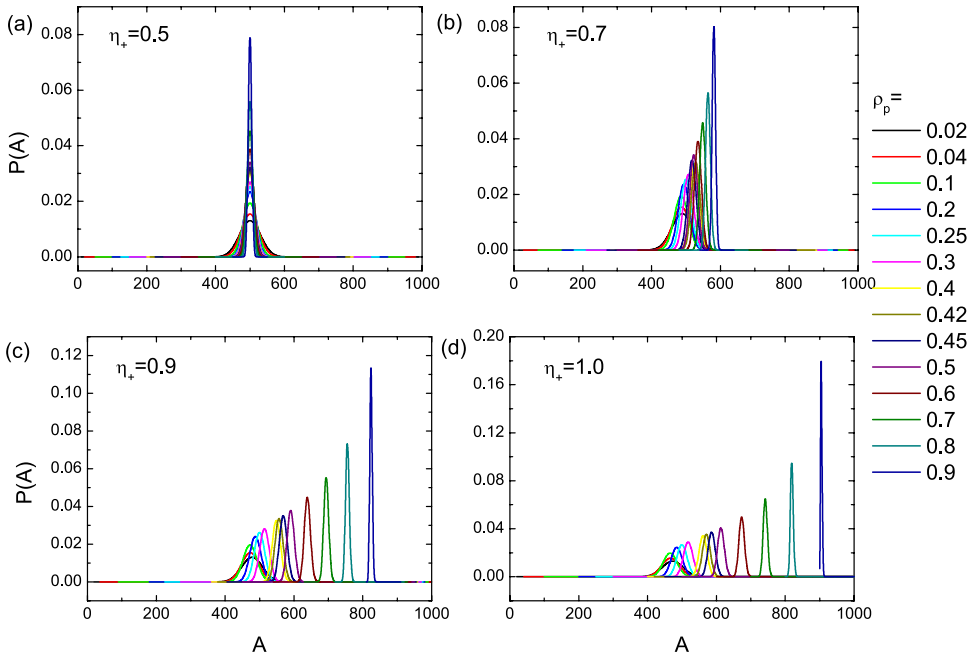

Figure 3. Theoretical prediction of the probability density distribution of attendance *A*. The distribution $P(A)$ is obtained from the transition matrix Eq. (7) for $N = 1001$. The value of the pinning pattern indicator η_+ is set as 0.5, 0.7, 0.9 and 1.0 in (**a**–**d**), respectively, and the pinning fraction ρ_p ranges from 0.02 to 0.9.

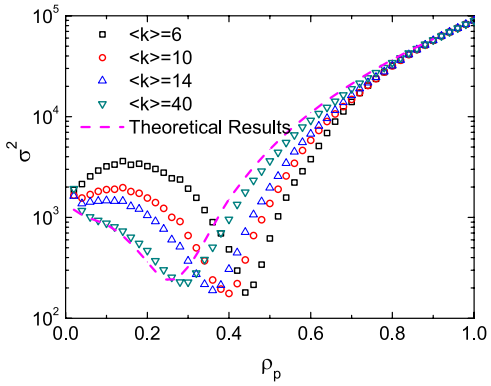

Figure 4. Theoretical prediction of the variance σ^2 in comparison with the simulation results. The system has size $N = 1001$ and power-law degree distribution $P(k)$ with scaling exponent $\gamma = 3$. The theoretical prediction does not depend on the value of the average degree. In direct simulations, the values of the average degree are $\langle k \rangle = 6$, 10, 14, and 40. The simulation results denoted by symbols are the same as those plotted in Fig. 1, with the pinning pattern indicator to be $\eta_+ = 0.8$.

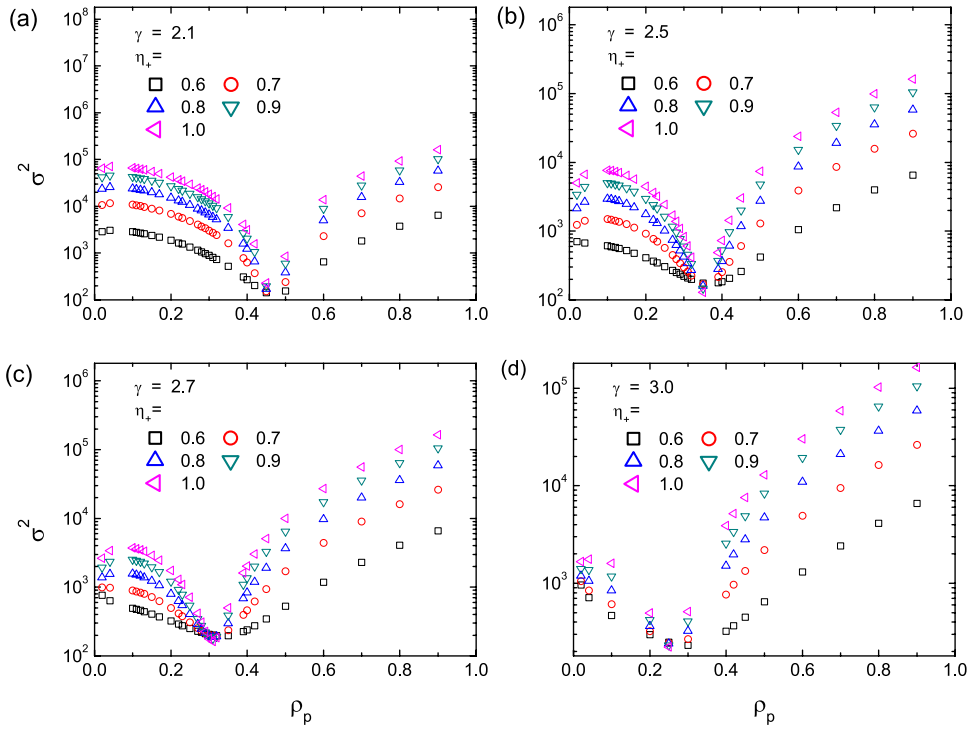

Figure 5. Theoretical prediction of variance σ^2 for systems with different degree scaling exponents. The system has size $N = 1001$ and power-law degree distribution $P(k)$ with different values of the degree exponent: (**a**–**d**) $\gamma = 2.1$, 2.5, 2.7, 3.0, respectively. In each case, the value of the pinning pattern indicator η_+ ranges from 0.6 to 1.0.

$$P(k, t+1|i, t) = \binom{N_f}{k - N_p\eta_+} \times \left(P_p\eta_- + P_f\frac{N_f - (i - N_p\eta_+)}{N_f}\right)^{k-N_p\eta_+} \times \left(P_p\eta_+ + P_f\frac{i - N_p\eta_+}{N_f}\right)^{N_f-(k-N_p\eta_+)}, \quad (6)$$

where $P_p\eta_- + P_f[N_f - (i - N_p\eta_+)]/N_f$ is the probability for a free agent to choose $+$ with the first and second terms representing the contributions of the pinned $-$ and free $-$ neighbors, respectively. In the Boolean system,

the values of attendance A oscillate about its equilibrium value[11]. The transition probability between the state at t and $t + 2$ can be expressed as a function of η_+:

$$\begin{aligned} T(j, i) &\equiv P(j, t+2|i, t) \\ &= \sum_k P(j, t+2|k, t+1) \cdot P(k, t+1|i, t) \\ &= \sum_k \left\{ \left[\binom{N_f}{k - N_p\eta_+} \times \left(P_p\eta_- + P_f \frac{N_f - i + N_p\eta_+}{N_f} \right)^{k - N_p\eta_+} \right. \right. \\ &\quad \left. \times \left(P_p\eta_+ + P_f \frac{i - N_p\eta_+}{N_f} \right)^{N_f - (k - N_p\eta_+)} \right] \\ &\quad \times \left[\binom{N_f}{j - N_p\eta_+} \times \left(P_p\eta_- + P_f \frac{N_f - k + N_p\eta_+}{N_f} \right)^{j - N_p\eta_+} \right. \\ &\quad \left. \left. \times \left(P_p\eta_+ + P_f \frac{k - N_p\eta_+}{N_f} \right)^{N_f - (j - N_p\eta_+)} \right] \right\}. \end{aligned} \tag{7}$$

Equation (7) takes into account the effect of pinning patterns, which was ignored previously[11]. The resulting balance equation governing the dynamics of the Markov chains becomes

$$P(j) = \sum_i P(j, t+2|i, t) P(i) \equiv \sum_i T(j, i) P(i), \tag{8}$$

which is the discrete-time master equation. The stable state that the system evolves into can be defined in the matrix form as

$$\boldsymbol{P}_A = \mathbb{T}\boldsymbol{P}_A, \tag{9}$$

where $\mathbb{T}$ is an $(N+1) \times (N+1)$ matrix with elements $\mathbb{T}_{ji} = T(j, i)$, and $\boldsymbol{P}_A$ is the corresponding vector of $P(A)$ with A ranging from 0 to N.

The probability distribution $P(A)$ is a binomial function with various expectation values, as shown in Fig. 3. In addition, the probability $P(A)$ is zero for $A \in [0, N_p\eta_+] \cup [N_p(1-\eta_+), N]$, which defines the boundary condition in the sense that there are $N_p = N \cdot \rho_p$ pinned agents. Once the stable distribution $P(A)$ is obtained from Eq. (9), the cumulative variance of the system can be calculated from

$$\sigma^2 = \sum_{A=0}^{N} P(A)(A - C_+)^2. \tag{10}$$

The theoretical prediction of σ^2 as a function of ρ_p can thus be made through (*a*) identifying the function $P_p(\rho_p)$, (*b*) defining the matrix $\mathbb{T}$ that depends on η_+ and $P_p(\rho_p)$, and (*c*) calculating the stable state $P(A)$.

Effect of network topology on pinning control. The topology of the network system has an effect on the probability P_p. For the particular case of scale-free networks with degree exponent $\gamma = 3$, our previous work[11] demonstrated that preferential pinning of the large-degree agents leads to $P_p = \sqrt{\rho_p}$. Here, we consider systems with degree distribution $P(k) = (\gamma - 1)/(k_{\min}^{1-\gamma} k^{\gamma})$, where $k_{\min}$ is the minimum degree of the network. For the DPP scheme where pinning occurs in the order from large to small degree agents, the relation between the minimum degree of *pinned* agents (denoted by k') and the pinning fraction ρ_p is

$$\rho_p(k') = \int_{k'}^{k_{\max}} P(k)\mathrm{d}k. \tag{11}$$

For a given pinning fraction $\rho_p(k')$ in which all the agents with $k > k'$ are pinned, the probability P_p for one neighbor of a given *free* agent to be a pinned agent is given by

$$P_p(k') = \frac{\int_{k'}^{k_{\max}} kP(k)\mathrm{d}k}{\int_{k_{\min}}^{k_{\max}} kP(k)\mathrm{d}k}. \tag{12}$$

Here, Eqs. (11) and (12) are applicable to the DPP scheme on networks of any degree distribution $P(k)$ without degree correlation. The underlying assumption in Eq. (12) is that the degrees of the neighboring agents are not correlated, i.e., the neighbors of the pinned agents obey the same degree distribution $P(k)$ of the whole system. For a scale-free network, P_p as a function of ρ_p can be expressed as

$$P_p(\rho_p) = \left(\frac{k'}{k_{\min}}\right)^{2-\gamma} = \rho_p^{\frac{2-\gamma}{1-\gamma}}. \tag{13}$$

For the special case of $\gamma = 3$, Eq. (13) reduces to the specific relationship obtained earlier[11]: $P_p(\rho_p) = \sqrt{\rho_p}$. As indicated by Eqs. (7–10), the specific form of matrix $\mathbb{T}$ with respect to ρ_p can be obtained by substituting Eq. (13) into Eq. (7), leading to the distribution $P(A)$ and finally the variance of the system σ^2 as a function of ρ_p. Figure 4 displays the theoretical predicted σ^2 (dashed curves) for various values of the pinning fraction ρ_p and of the pinning pattern indicator η_+. The trend and, more importantly, the existence of the optimal pinning fraction ρ_p^*, agree well with the simulation results (marked with different symbols). In the limit $\langle k\rangle \to \infty$, the system approaches a well-mixed state that can be fully characterized by Eq. (13), indicating that the simulation results approach the curve predicted by the mean-field theory as the average degree $\langle k\rangle$ is increased.

Figure 5 shows the theoretical prediction of σ^2 for scale-free networks with different values of the degree exponent γ, which agrees well with the results from direct simulation as in Fig. 2. For the case of highly heterogeneous networks ($\gamma = 2.1$), the theoretical prediction deviates slightly from the numerical results for the reason that the networks in simulation inevitably exhibit certain topological features that are not taken into account in the theoretical analysis of $P_p(\rho_p)$, such as the degree correlation.

Optimal pinning. Our analysis based on the master equation (8) applies to systems with $F_{+|-} = F_{-|+} = 1$ and identical resource capacity. We now consider the more general case of varying $\mathbb{F}$ values to further understand the optimal pinning control scheme.

Deviation of expected attendance from resource capacity. The dependence of A^* on η_+ can be obtained through the general form of the response matrix $\mathbb{F}$. For convenience, we use the column vector $\hat{\eta} = (\eta_+, \eta_-)^{\mathrm{T}}$ to denote the fraction of the agents pinned at $+$ and $-$, where $\eta_+ + \eta_- = 1, \hat{\omega} = (\omega_+, \omega_-)^{\mathrm{T}}$ is the fraction of free agents adopting states $+$ and $-$, respectively, with $\omega_+ + \omega_- = 1$. The state of the system can be expressed as $\hat{\rho}(t) = \rho_p\hat{\eta} + \rho_f\hat{\omega}(t)$, from which we have

$$\hat{\omega}(t) = [\hat{\rho}(t) - \rho_p\hat{\eta}]/\rho_f, \tag{14}$$

At the next time step, the expected value of the state based on $\hat{\rho}(t)$ through the response matrix $\mathbb{F}$ can be written as

$$\hat{\rho}(t+1) = \rho_p\hat{\eta} + \rho_f[P_p\mathbb{F}\hat{\eta} + P_f\mathbb{F}\hat{\omega}(t)]. \tag{15}$$

Substituting Eq. (14) into Eq. (15), we get the relationship between $\hat{\rho}(t+1)$ and $\hat{\rho}(t)$. A self-consistency process stipulated by Eqs. (14) and (15) can yield the stable state of the system with the expected number of agents choosing $+$ given by

$$A^* = N\frac{F_{+|-}(\rho_p - 1) - \rho_p\eta_+(F_{+|-} + F_{-|+}) + \eta_+P_p(F_{+|-} + F_{-|+} - 1)}{P_p(F_{+|-} + F_{-|+} - 1) - (F_{+|-} + F_{-|+})}. \tag{16}$$

In a free system without pinning, the rational response $\mathbb{F}$ of agents to nonidentical capacities of resources leads to Eq. (3), implying the relationship $C_+ = NF_{+|-}/(F_{+|-} + F_{-|+})$. From Eq. (16), we can obtain ε as a function of the value of the pinning pattern indicator η_+, the elements of the matrix $\mathbb{F}$, the pinning fraction ρ_p, and the parameter P_p associated with network topology. We have

$$\begin{aligned}\varepsilon \;=\; A^* - C_+ = N\cdot[F_{+|-}(\eta_+ - 1) + F_{-|+}\eta_+]\cdot \\ \frac{[\rho_p(F_{+|-} + F_{-|+}) - P_p(F_{+|-} + F_{-|+} - 1)]}{(F_{+|-} + F_{-|+})\cdot[F_{+|-} + F_{-|+} - (F_{-|+} + F_{-|+} - 1)P_p]},\end{aligned} \tag{17}$$

which has the form of separated variables associated with η_+ and ρ_p.

Optimal pinning pattern and fraction. Optimizing the system requires minimum $X_2(\varepsilon)$, i.e., $\varepsilon = 0$ in Eq. (17), leading to two independent solutions:

$$\frac{\eta_+^*}{\eta_-^*} = \frac{F_{+|-}}{F_{-|+}} = \frac{C_+}{C_-}, \tag{18a}$$

$$P_p(\rho_p^*) = \frac{F_{+|-} + F_{-|+}}{F_{+|-} + F_{-|+} - 1}\rho_p^*, \tag{18b}$$

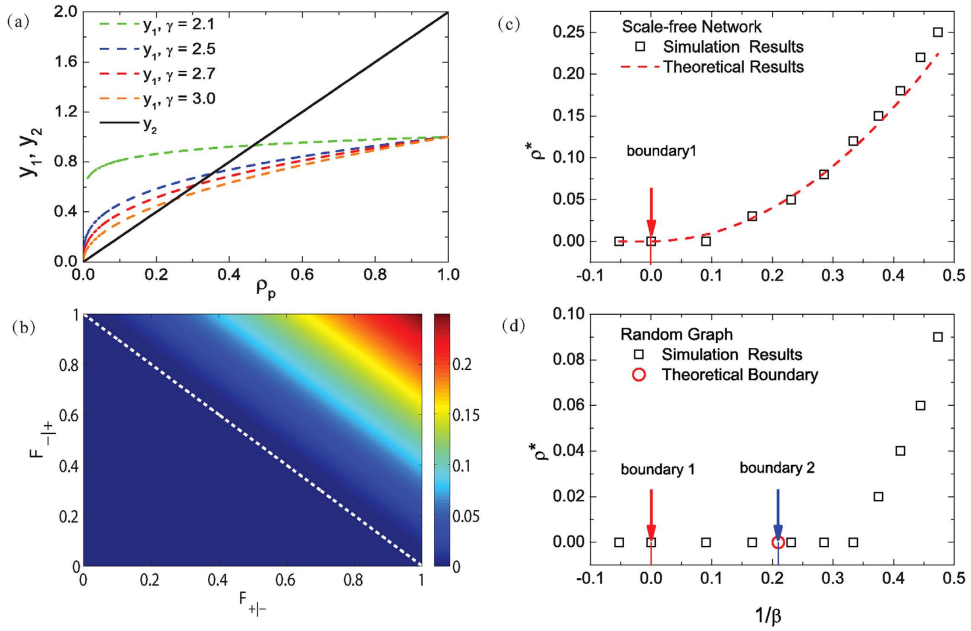

Figure 6. Optimal pinning fraction. (**a**) Intersections of the curves $y_1 = P_p(\rho_p)$ and $y_2 = \beta \cdot \rho_p$ denote nonzero optimal pinning fraction ρ_p^* given by Eq. (18b). The scale-free networks have the degree exponents $\gamma = 2.1, 2.5, 2.7$, and 3.0, respectively. The response function is for $F_{+|-} = F_{-|+} = 1$ (corresponding to $C_+ = C_-$). (**b**) Contour map of ρ_p^* in the parameter space of $F_{+|-}$ and $F_{-|+}$ for scale-free networks with $\gamma = 3$. In the lower-left region below the boundary $F_{+|-} + F_{-|+} = 1$ (white dashed line), nonzero solution of ρ_p^* cannot be obtained. (**c**) Optimal pinning fraction ρ_p^* as a function of $1/\beta$ for scale-free networks. The analytical results from Eq. (18b) (red solid curve) and the simulation results (black open squares) agree well with each other. The red arrow marks the theoretical prediction of the boundary, where nonzero ρ_p^* solutions exist on the left side. (**d**) For ER random networks, ρ_p^* as a function of $1/\beta$. Theoretical results from Eq. (18b) (red open circle) and simulation results (black open squares) are shown. The boundaries 1 and 2 obtained theoretically (pointed to by solid arrows), respectively, stand for the constraint in Eqs. (19) and (22). In (**c**,**d**), the value of $F_{-|+}$ varies but $F_{+|-}$ is set to 0.9. The scale-free and random networks used in the simulations have $\langle k \rangle = 40$ and $N = 2001$.

which respectively correspond to the optimal value of the pinning pattern indicator η_+^* and the optimal pinning fraction ρ_p^*. Here, for convenience, we define a parameter: $\beta \equiv (F_{+|-} + F_{-|+})/(F_{+|-} + F_{-|+} - 1)$ so that Eq. (18b) can be expressed concisely as $P_p(\rho_p^*) = \beta \cdot \rho_p^*$. Once the values of η_+ and ρ_p satisfy either Eq. (18a) or Eq. (18b), we can obtain $X_2(\varepsilon) = 0$. The variance σ^2 depends on the fluctuation factor $X_1(\delta)$ only.

Equation (18a) specifies the pinning pattern with the same ratio as that of the resource capacity. The Boolean dynamics studied previously[11] is a special case where the optimal pinning pattern indicator is $\eta_+^*/\eta_-^* = 1$ (i.e., $\eta_+^* = 0.5$) for systems with $C_+ = C_-$, and the variance σ^2 is simply determined by the factor $X_1(\delta)$ alone.

From Eq. (18b), we see that the optimal pinning fraction ρ_p^* is independent of η_+ but depends on both the network structure through $P_p(\rho_p)$ and on the response function $\mathbb{F}$. Additionally, the condition $\rho_p \in [0, 1]$ and nonzero denominator require

$$F_{+|-} + F_{-|+} - 1 > 0. \tag{19}$$

The function $P_p(\rho_p)$ for scale-free networks, as in Eq. (13), increases monotonically with ρ_p. Figure 6(a) displays the curves $y_1 = P_p(\rho_p)$ and $y_2 = \beta \cdot \rho_p$, i.e., both sides of Eq. (18b). The existence of nonzero ρ_p^* for $y_1 = y_2$ demands

$$\left.\frac{dP_p(\rho_p)}{d\rho_p}\right|_{\rho_p=0} > \beta. \tag{20}$$

For scale-free networks, $P_p(\rho_p)$ diverges at ρ_p=0. Equation (20) thus holds, implying that the DPP pinning scheme has a nonzero optimal pinning fraction ρ_p^*, leading to $\varepsilon = 0$. However, for homogeneous networks, Eq. (20) may not hold. In this case, a more specific implicit condition can be obtained from Eq. (20) through the

following analysis. In particular, without an analytical expression of $P_p(\rho_p)$, the derivative of $P_p(\rho_p)$ with respect to ρ_p can be obtained from Eqs. (11) and (12):

$$\frac{dP_p(\rho_p)}{d\rho_p} = \frac{dP_p(k')}{dk'} \cdot \frac{dk'}{d\rho_p(k')} = \frac{k'P(k')}{\langle k\rangle P(k')} = \frac{k'}{\langle k\rangle}. \tag{21}$$

For degree preferential pinning, in the limit $\rho_p \to 0$, the maximum degree for *free* agents is $k' \to k_{\max}$. We thus have

$$\left.\frac{dP_p(\rho_p)}{d\rho_p}\right|_{\rho_p=0} = \frac{k_{\max}}{\langle k\rangle} > \beta, \tag{22}$$

which requires that the network be heterogeneous. For $F_{+|-} = F_{-|+} = 1$, we have $k_{\max}/\langle k\rangle > 2$, ensuring the existence of a nonzero ρ_p^* value for $\varepsilon = 0$.

The contour map of the optimal pinning fraction ρ_p^* in the parameter space of $F_{+|-}$ and $F_{-|+}$ for scale-free networks with $\gamma = 3$ is shown in Fig. 6(b). The boundary $F_{+|-} + F_{-|+} = 1$ associated with condition Eq. (19) is represented by the white dashed line, where nonzero solutions of ρ_p^* do not exist below the lower-left region. Figure 6(c,d) show ρ_p^* for $\varepsilon = 0$ as a function of $1/\beta$ for scale-free and random networks, respectively, where $F_{-|+}$ is varied and $F_{+|-}$ is fixed to 0.9. The theoretical prediction of ρ_p^* [red solid curve in (c) and red open circle in (d)] is given by the intersections of the curves y_1 and y_2 in Fig. 6(a). For scale-free networks, since Eq. (20) holds, Eq. (21) is the only constraint on the value of $1/\beta$ (red dashed arrow), with the region at the right-hand side yielding nonzero ρ_p^* solutions. The red solid curve in Fig. 6(c) represents the theoretical prediction, and the open squares denote the simulation results from scale-free networks of size $N = 2001$, power-law exponent $\gamma = 3$, and average degree $\langle k\rangle = 40$.

For random networks, the existence of nonzero ρ_p^* solutions requires that Eqs. (19) and (21) or (22) hold. For the Poisson degree distribution, the maximum degree of the network can be calculated from

$$\frac{e^{-k_{\max}}\langle k\rangle}{k_{\max}!} \approx \frac{1}{N}. \tag{23}$$

We can obtain an estimate of the value of $1/\beta$ that satisfies Eq. (22), as indicated by the blue arrow (labeled as boundary 2) in Fig. 6(d). The right-hand side of this point satisfies both Eqs. (19) and (22), implying the existence of nonzero ρ_p^*. Comparison of the results from random and scale-free networks with different scaling exponents (Figs 2,5 and 6) shows that, stronger heterogeneity tends to enhance the values of ρ_p^*, which can also be seen from Eq. (20).

To better understand the non-monotonic behavior of σ^2 with ρ_p, we provide a physical picture of the behavioral change for ρ_p greater or less than ρ_p^*. The effect of pinning control is determined by the number of edges between pinned and free agents, which are *pinning-free edges*. For a small pinning fraction ρ_p, the average effect per pinned agent on the system (represented by the number of pinned-free edges per pinned agent) is relatively large. However, as ρ_p is increased, the average impact is reduced for two reasons: (*a*) an increase in the edges within the pinned agents' community itself (i.e., two connected pinned agents), which has no effect on control, and (*b*) a decrease in the number of free agents, which directly reduces the number of pinned-free edges. Consider the special case of $\eta_+ = 1$ and $C_+ = C_-$. For small ρ_p, the pinned $+$ agents have a significant impact so that the free agents tend to overestimate the probability of winning by adopting $-$. In this case, the expected value A^* is smaller than $0.5N$, corresponding to $\varepsilon < 0$. For highly heterogeneous systems, the average impact per pinned agent is larger for a given small value of ρ_p. As ρ_p is increased, the average influence per pinned agent reduces and, consequently, A^* restores towards $0.5\,N$. For $A^* = 0.5\,N$ and $\varepsilon = 0$, the system variance [Eq. (5)] is minimized due to $X_2(\varepsilon) = 0$, and the corresponding pinning fraction achieves the optimal value ρ_p^*. For strongly heterogeneous systems, due to the large initial average impact caused by pinning the hub agents, the optimal pinning fraction ρ_p^* appears in the larger ρ_p region. Further increase in ρ_p with $\eta_+ = 1$ will lead to $\varepsilon > 0$ and $A^* > 0.5N$, thereby introducing nonzero $X_2(\varepsilon)$ again and, consequently, generating an increasing trend in σ^2.

Collapse of variance. For certain networks, the variance $\sigma^2(\eta_+, \rho_p)$ is determined by the values of the pinning pattern indicator η_+ and the pinning fraction ρ_p. Our analysis so far focuses on the contribution of $X_2(\varepsilon)$ to the variance σ^2 as the pinning fraction ρ_p is increased but for fixed η_+. It is thus useful to define a quantity related to the variance σ^2, which can be expressed in the form of separated variables. For two different values of the pinning pattern indicator, η_+ and η_+', for a given value of ρ_p, the relative weight of $X_2(\varepsilon)$ can be obtained from Eq. (17) as

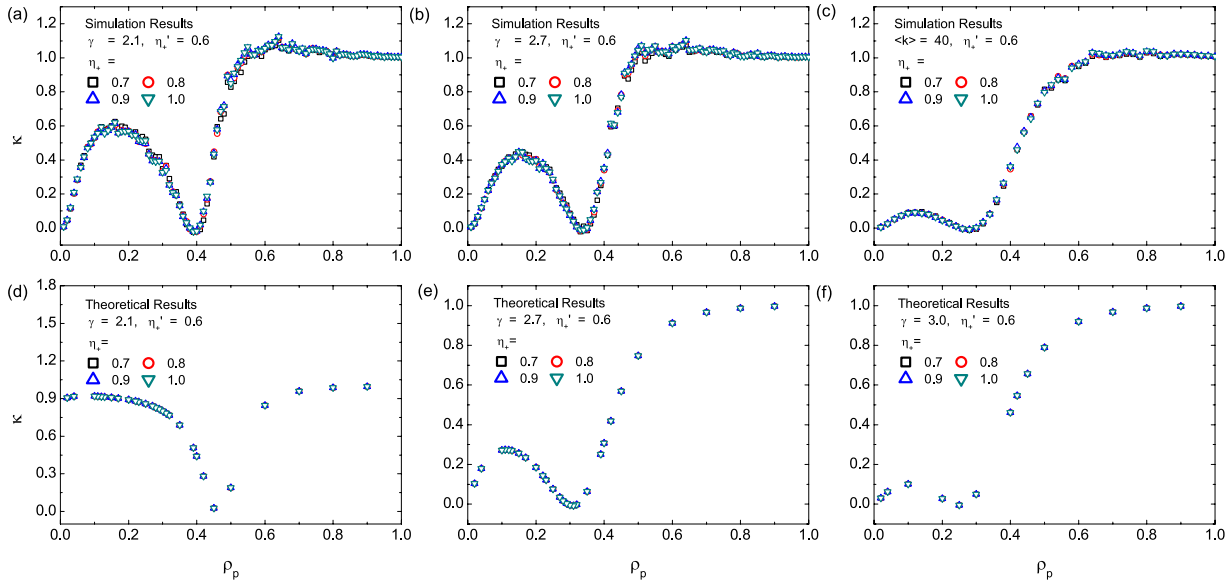

Figure 7. Collapse of κ for different pinning patterns. (**a–c**) Simulation results of κ from scale-free networks for $\gamma = 2.1$, 2.7, and 3.0, which correspond to the results of σ^2 in Figs 1(d) and 2(a,c), respectively. (**d–f**) Theoretical results of κ from Eq. (27) for the cases shown in Fig. 5(a,c,d), respectively. The reference pinning pattern indicator is $\eta' = 0.6$.

$$\lambda(\eta_+, \eta_+', \rho_p) \equiv \frac{X_2(\varepsilon(\eta_+, \rho_p))}{X_2(\varepsilon(\eta_+', \rho_p))} = \left[\frac{\varepsilon(\eta_+, \rho_p)}{\varepsilon(\eta_+', \rho_p)}\right]^2 = \left[\frac{F_{+|-}(\eta_+ - 1) + F_{-|+}\eta_+}{F_{+|-}(\eta_+' - 1) + F_{-|+}\eta_+'}\right]^2, \tag{24}$$

where $\varepsilon(\eta_+, \rho_p)$ is a function of both η_+ and ρ_p. Remarkably, the ratio λ depends on η_+ and η_+' but it is independent of ρ_p, due to the form of separated variables in Eq. (17). From the simple relationship Eq. (24), we can define the relative changes in these quantities due to an increase in the value of η_+ from a *reference value* η_+' as

$$\Pi(\eta_+, \eta_+', \rho_p) \equiv \frac{\sigma^2(\eta_+, \rho_p) - \sigma^2(\eta_+', \rho_p)}{\sigma^2(\eta_+', \rho_p)}, \tag{25}$$

$$\Omega(\eta_+, \eta_+') \equiv \frac{X_2(\varepsilon(\eta_+)) - X_2(\varepsilon(\eta_+'))}{X_2(\varepsilon(\eta_+'))}, \tag{26}$$

and then obtain the change rate associated with σ^2 and $X_2(\varepsilon)$ as,

$$\kappa(\eta_+, \eta_+', \rho_p) = \Pi(\eta_+, \eta_+', \rho_p)/\Omega(\eta_+, \eta_+'), \tag{27}$$

where $\Omega(\eta_+, \eta_+')$ is independent of ρ_p. In the limit $(\eta_+ - \eta_+') \to 0$, the rate of change $\kappa(\eta_+, \eta_+', \rho_p)$ becomes

$$\kappa(\eta_+', \rho_p) = \frac{\partial \ \ln[\sigma^2(\eta_+', \rho_p)]}{\partial \eta_+'} \Big/ \frac{d \ \ln[X_2(\varepsilon(\eta_+'))]}{d\eta_+'}. \tag{28}$$

Figure 7 shows $\kappa(\eta_+', \rho_p)$ as a function of ρ_p for scale-free networks, where the value of the reference pinning pattern indicator is $\eta_+' = 0.6$. To obtain the values of κ, we first calculate Ω by substituting the values of η_+, η_+' and the elements of $\mathbb{F}$ into Eqs. (24) and (26). We then obtain Π by substituting the values of σ^2 into Eq. (25), with σ^2 either from simulation as in Figs 1 and 2 or from theoretical analysis as in Fig. 5. We see that the κ values from simulation results of σ^2 [Fig. 7(a–c) marked by "Simulation Results"] and theoretical prediction of σ^2 [Fig. 7(d–f) marked by "Theoretical Results"] show the behavior in which the curves of κ for different values of η_+ collapse into a single one. This indicates that κ depends solely on the pinning fraction ρ_p; it is independent of the value of the pinning pattern indicator η_+. Extensive simulations and analysis of scale-free networks with different average degree $\langle k \rangle$ or different degree exponent γ verify the generality of the collapsing behavior.

From Eq. (28), we see that the variance $\sigma^2(\eta_+, \rho_p)$ and the quantity κ are closely related. For example, a smaller value of κ indicates that $X_2(\varepsilon)$ contributes more to the variance of $\sigma^2(\eta_+, \rho_p)$ as η_+ is changed, and vice versa. In

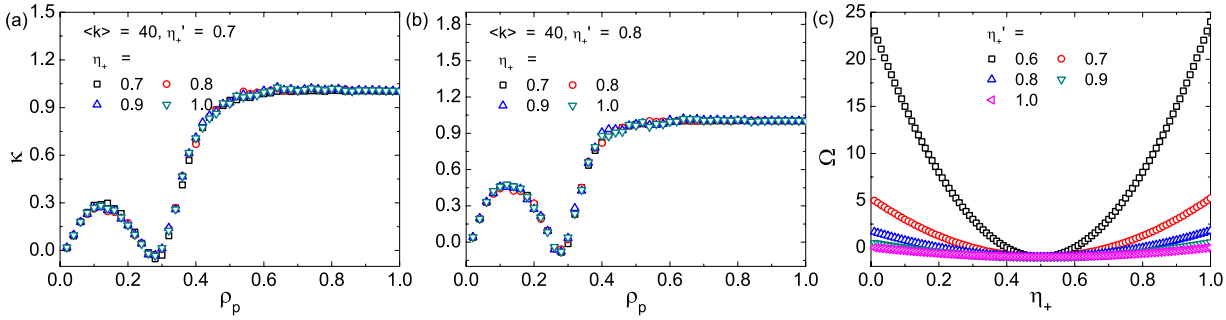

Figure 8. Two separated functions κ and Ω in Eq. (29). (**a**,**b**) Collapse of $\kappa(\rho_p)$ for various η_+ values, where the reference value is $\eta_+' = 0.7$ in (**a**) and 0.8 in (**b**). The values of κ are predicted from Eq. (27) for a scale-free network with $\gamma = 3$ and $\langle k \rangle = 40$. (**c**) The function $\Omega(\eta_+)$ for $\eta_+' = 0.6, 0.7, 0.8, 0.9, 1.0$, and $F_{+|-} = F_{-|+} = 1$.

Fig. 7, $\kappa = 0$ corresponds to the intersecting points of the curves of σ^2 with different values of η_+ shown in Figs 1,2 and 5. It can also be verified analytically that, the minimal point with $\partial\kappa/\partial\rho_p = 0$ coincides with the optimal pinning fraction ρ_p^* at which σ^2 is minimized, which is supported by simulation results in Figs 1,2,5 and 7.

Variance in the form of separated variables. From Eq. (27), for a given value of the reference pinning pattern indicator η_+', we can obtain an expression of Π in the form of separated variables as

$$\Pi(\eta_+, \rho_p) = \kappa(\rho_p) \cdot \Omega(\eta_+), \tag{29}$$

where $\kappa(\rho_p)$ is independent of the change in η_+, and $\Omega(\eta_+)$ is independent of ρ_p. The consequence of Eq. (29) is remarkable, since it defines in the parameter space (η_+, ρ_p) a function Π in the form of separated variables which, as compared with the original quantity σ^2, not only simplifies the description but also gives a more intuitive picture of the system behavior. Specifically, for the MG dynamics, the influences of various factors on the variance σ^2 or $\Pi(\eta_+, \rho_p)$ can be classified into two parts: (I) the function κ that reflects the effects of the pinning fraction ρ_p and the network structure among agents (in terms of the degree distribution $P(k)$, the average degree $\langle k \rangle$, and the scaling exponent γ), and (II) the function Ω that characterizes the impact of the pinning pattern indicator η_+ and the response of agents to resource capacities C_+ and C_- through $\mathbb{F}$. Figure 8(a,b) show the values of κ as a function of ρ_p for $\eta_+' = 0.7$ and 0.8, respectively, whereas Fig. 8(c) shows $\Omega(\eta_+)$ for several values of η_+'. From Eqs (24) and (26), we see that Ω is a quadratic function of η_+ with the symmetry axis at $\eta_+ = F_{+|-}/(F_{+|-} + F_{-|+})$, which depends on the setting of response function $\mathbb{F}$. The second derivative of the function depends on η_+'.

From the definition in Eq. (25), the variance of the system for arbitrary values of ρ_p and η_+ can be obtained as

$$\sigma^2(\eta_+, \rho_p) = [\kappa(\rho_p) \cdot \Omega(\eta_+) + 1] \cdot \sigma^2(\eta_+', \rho_p), \tag{30}$$

where η_+' specifies the reference pinning pattern. Once we have the two respective $\sigma^2(\eta_+, \rho_p)$ curves for the two specific pinning patterns as specified by η_+' and η_+'', σ^2 in the whole parameter space (η_+, ρ_p) can be calculated accordingly. In particular, the quantities $\sigma^2(\eta_+', \rho_p)$ and $\sigma^2(\eta_+'', \rho_p)$ serve as a *holographic* representation of the dynamical behavior of the system in the whole parameter space. In particular, one can first obtain $\Omega(\eta_+)$ from Eqs (17) and (26), and then calculate $\kappa(\rho_p) = \Pi(\eta_+'', \rho_p)/\Omega(\eta_+'')$, and finally obtain the value of $\sigma^2(\eta_+, \rho_p)$ by substituting $\Omega(\eta_+)$ and $\kappa(\rho_p)$ into Eq. (30).

Analysis of Gini index. The equality of wealth is also an important criterion to assess the performance of a resource allocation system, which can be characterized by the Gini index. For MG systems without control, it was found that inequality in wealth can be pronounced when the resource utility is optimized[63]. We calculate the Gini index to uncover the interplay between pinning control and wealth equality in Boolean systems. In particular, the Gini index is defined as

$$G_0 = 1 - \frac{1}{N}\sum_{j=1}^{N}[1 + 2(N - j)]g_j, \tag{31}$$

where N is the total number of agents in the system and g_j is the ratio of the wealth earned by agent j over the total amount of wealth in the whole system. Note that g_j is ranked in the ascending order as $g_1 \le g_2 \le \cdots \le g_N$. During each round of the game (each time step), the wealth of each minority agent is set to increase by one unit, while the wealth of the majority agents is unchanged. The accumulated wealth of each agent over a long time interval (e.g., $T = 500$ time steps) can be used to calculate the Gini index of the system according to its definition. Figure 9 shows the value of the Gini index G_0 as a function of ρ_p, where panels (a–c) are the results for scale-free

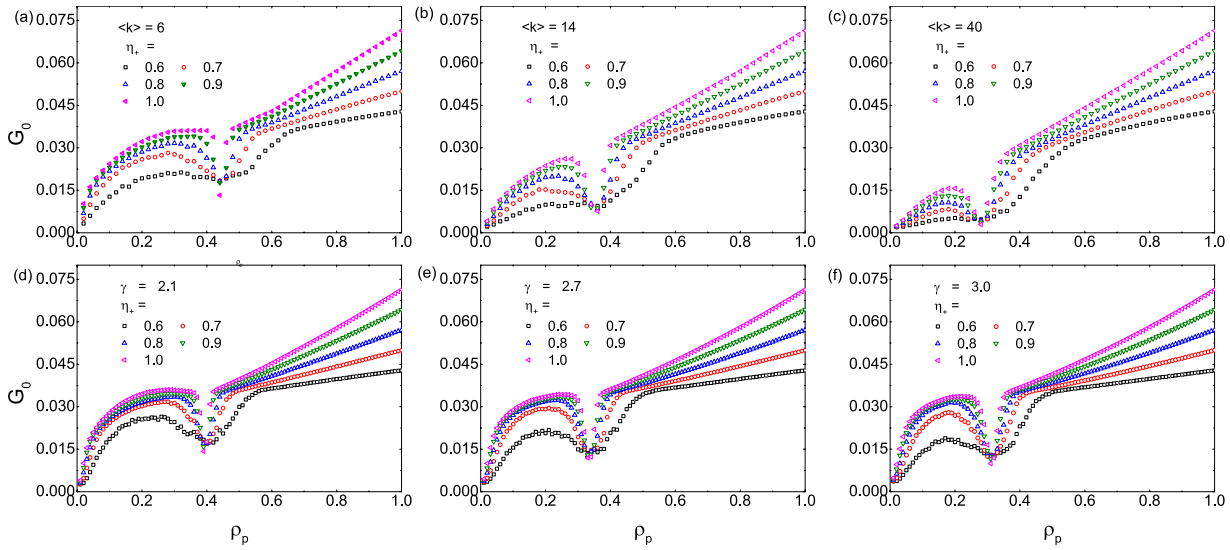

Figure 9. Gini index G_0 as a function of the pinning fraction ρ_p. (**a**–**c**) Results obtained from scale-free networks with degree scaling exponent $\gamma = 3.0$[54], system size $N = 1001$, and average degree $\langle k \rangle = 6$, 14 and 40, respectively. (**d**–**f**) Results from scale-free networks[55] of size $N = 2001$ and degree scaling exponent $\gamma = 2.1$, 2.7, and 3.0, respectively. The value of the pinning pattern indicator η_+ ranges from 0.6 to 1.0.

networks[54] of scaling exponent $\gamma = 3.0$ and system size $N = 1001$, and for three different values of the average degree: $\langle k \rangle = 6$, 14 and 40, respectively. Results for scale-free networks[55] of size $N = 2001$ and three different values of the scaling exponent: $\gamma = 2.1$, 2.7, and 3.0, are shown in panels (d–f), respectively. In each panel, the value of the pinning pattern indicator η_+ ranges from 0.6 to 1.0. In reference to the variance σ^2 in Figs 1 and 2 for the same networks under identical dynamical parameter setting, we see that the value of G_0 reaches a local minimum at the optimal pinning fraction ρ_p^*. This implies that optimal use of resources and equality in wealth in a population can be realized simultaneously through pinning control.

As shown in each panel of Fig. 9, for larger values of η_+ (i.e., larger biases in pinning), the value of G_0 is generally larger and more sensitive to changes in the pinning fraction ρ_p, i.e., G_0 varies more rapidly with ρ_p. When the system's utilization of resource is optimized at ρ_p^*, we have $\sigma^2 = \delta^2$ (because $\varepsilon^2 = 0$ - see Eq. (5) and discussions). We see that the Gini index can be determined through the fluctuation δ^2 of $A(t)$. As a result, if the pinning scheme is more biased (a larger value of η_+), the fluctuations of $A(t)$ are smaller, leading to a smaller value of G_0. In addition, for the scale-free networks with larger average degree $\langle k \rangle$, G_0 increases more rapidly as ρ_p is increased from zero.

Discussions

The phenomenon of herding is ubiquitous in social and economical systems. Herding behavior may play a positive role in certain types of dynamical processes, with examples such as promoting cooperation in evolutionary game dynamics[64–66] and encouraging vaccination to prevent or suppress epidemic spreading[67]. However, in systems that involve and/or rely on fair resource allocation, the emergence of herding behavior is undesirable, as in such a state a vast majority of the individuals in the system share only a few resources, a precursor of system collapse at a global scale. A generic manifestation of herding behavior is relatively large fluctuations in the dynamical variables of the system such as the numbers of individuals sharing certain resources. It is thus desirable to develop effective control methods to suppress herding. An existing and powerful mathematical framework to model and understand the herding behavior is minority games. Investigating control of herding in the MG framework may provide useful insights into developing more realistic control method for real-world systems.

Built upon our previous works in MG systems[4,11], in this paper we articulate, test, and analyze a general pinning scheme to control herding behavior in MG systems. A striking finding is the universal existence of an optimal pinning fraction that minimizes the variance and realizes the equality among the agents in the system, regardless of system details such as the degree of homogeneity of the resource capacities, topology and structures of the underlying network, and different patterns of pinning. This means that, generally, the efficiency of the system can be optimized for some relatively small pinning fraction. Employing the mean-field approach, we develop a detailed theory to understand and predict the dynamics of the MG system subject to pinning control, for various network topologies and pinning schemes. The key observation underlying our theory is the two factors contributing to the system fluctuations: intrinsic dynamical fluctuations and systematic deviation of agents' expected attendance from resource capacity. The theoretically predicted fluctuations (quantified by the system variance) agree with those from direct simulation. In particular, in the large degree limit, for a variety of combinations of the network and pinning parameters, the numerical results approach those predicted from our mean field theory. Our theory also correctly predicts the optimal pinning fraction for various system and control settings.

In real world systems in which resource allocation is an important component, resource capacities and agent interactions can be diverse and time dependent. To develop MG model to understand the effects of diversity and time dependence on herding dynamics, and to exploit the understanding to develop pinning control methods to suppress or eliminate herding are open issues at the present. Furthermore, implementation of pinning control in real systems may be associated with incentive policies that provide compensations or rewards to the pinned agents. How to reduce the optimal pinning fraction then becomes an interesting issue. Our results provide insights and represent a step toward the goal of designing highly stable and efficient resource allocation systems.

References

1. Paczuski, M., Bassler, K. E. & Corral, A. Self-organized networks of competing boolean agents. *Phys. Rev. Lett.* **84,** 3185–3188 (2000).
2. Vázquez, A. Self-organization in populations of competing agents. *Phys. Rev. E* **62,** R4497 (2000).
3. Galstyan, A. & Lerman, K. Adaptive boolean networks and minority games with time-dependent capacities. *Phys. Rev. E* **66,** 015103 (2002).
4. Zhou, T., Wang, B.-H., Zhou, P.-L., Yang, C.-X. & Liu, J. Self-organized boolean game on networks. *Phys. Rev. E* **72,** 046139 (2005).
5. Eguíluz, V. M. & Zimmermann, M. G. Transmission of information and herd behavior: An application to financial markets. *Phys. Rev. Lett.* **85,** 5659–5662 (2000).
6. Lee, S. & Kim, Y. Effects of smartness, preferential attachment and variable number of agents on herd behavior in financial markets. *J. Korean. Phys. Soc.* **44,** 672–676 (2004).
7. Wang, J. *et al.* Evolutionary percolation model of stock market with variable agent number. *Physica A* **354,** 505–517 (2005).
8. Zhou, P.-L. *et al.* Avalanche dynamics of the financial market. *New Math. Nat. Comp.* **1,** 275–283 (2005).
9. Huang, Z.-G., Wu, Z.-X., Guan, J.-Y. & Wang, Y.-H. Memory-based boolean game and self-organized phenomena on networks. *Chin. Phys. Lett.* **23,** 3119 (2006).
10. Huang, Z.-G., Zhang, J.-Q., Dong, J.-Q., Huang, L. & Lai, Y.-C. Emergence of grouping in multi-resource minority game dynamics. *Sci. Rep.* **2,** 703 (2012).
11. Zhang, J.-Q., Huang, Z.-G., Dong, J.-Q., Huang, L. & Lai, Y.-C. Controlling collective dynamics in complex minority-game resource-allocation systems. *Phys. Rev. E* **87,** 052808 (2013).
12. Dong, J.-Q., Huang, Z.-G., Huang, L. & Lai, Y.-C. Triple grouping and period-three oscillations in minority-game dynamics. *Phys. Rev. E* **90,** 062917 (2014).
13. Banerjee, A. V. A simple model of herd behavior. *Q. J. Econ.* 797–817 (1992).
14. Cont, R. & Bouchaud, J.-P. Herd behavior and aggregate fluctuations in financial markets. *Macroecon. Dyn.* **4,** 170–196 (2000).
15. Ali, S. N. & Kartik, N. Herding with collective preferences. *Econ. Theor.* **51,** 601–626 (2012).
16. Morone, A. & Samanidou, E. A simple note on herd behaviour. *J. Evol. Econ* **18,** 639–646 (2008).
17. Kauffman, S. A. *The origins of order: Self-organization and selection in evolution* (Oxford university press, 1993).
18. Levin, S. A. Ecosystems and the biosphere as complex adaptive systems. *Ecosystems* **1,** 431–436 (1998).
19. Arthur, W. B., Durlauf, S. N. & Lane, D. A. *The economy as an evolving complex system II*, vol. 28 (Addison-Wesley Reading, MA, 1997).
20. Challet, D. & Zhang, Y.-C. Emergence of cooperation and organization in an evolutionary game. *Physica A* **246,** 407–418 (1997).
21. Challet, D. *et al.* Minority games: interacting agents in financial markets. *OUP Catalogue* (2013).
22. Arthur, W. B. Inductive reasoning and bounded rationality. *Am. Econ. Rev.* **84,** 406–411 (1994).
23. Challet, D. & Marsili, M. Phase transition and symmetry breaking in the minority game. *Phys. Rev. E* **60,** R6271–R6274 (1999).
24. Challet, D., Marsili, M. & Zecchina, R. Statistical mechanics of systems with heterogeneous agents: Minority games. *Phys. Rev. Lett.* **84,** 1824–1827 (2000).
25. Martino, A. D., Marsili, M. & Mulet, R. Adaptive drivers in a model of urban traffic. *Europhys. Lett.* **65,** 283 (2004).
26. Borghesi, C., Marsili, M. & Miccichè, S. Emergence of time-horizon invariant correlation structure in financial returns by subtraction of the market mode. *Phys. Rev. E* **76,** 026104 (2007).
27. Savit, R., Manuca, R. & Riolo, R. Adaptive competition, market efficiency, and phase transitions. *Phys. Rev. Lett.* **82,** 2203 (1999).
28. Kalinowski, T., Schulz, H.-J. & Birese, M. Cooperation in the minority game with local information. *Physica A* **277,** 502 (2000).
29. Slanina, F. Harms and benefits from social imitation. *Physica A* **299,** 334–343 (2001).
30. Anghel, M., Toroczkai, Z., Bassler, K. E. & Korniss, G. Competition-driven network dynamics: Emergence of a scale-free leadership structure and collective efficiency. *Phys. Rev. Lett.* **92,** 058701 (2004).
31. Johnson, N. F., Hart, M. & Hui, P. M. Crowd effects and volatility in markets with competing agents. *Physica A* **269,** 1–8 (1999).
32. Hart, M., Jefferies, P., Johnson, N. F. & Hui, P. M. Crowd-anticrowd theory of the minority game. *Physica A* **298,** 537–544 (2001).
33. Lo, T. S., Chan, H. Y., Hui, P. M. & Johnson, N. F. Theory of networked minority games based on strategy pattern dynamics. *Phys. Rev. E* **70,** 056102 (2004).
34. Lo, T. S., Chan, K. P., Hui, P. M. & Johnson, N. F. Theory of enhanced performance emerging in a sparsely connected competitive population. *Phys. Rev. E* **71,** 050101 (2005).
35. Challet, D., Martino, A. D. & Marsili, M. Dynamical instabilities in a simple minority game with discounting. *J. Stat. Mech. Theory E.* **2008,** L04004 (2008).
36. Bianconi, G., Martino, A. D., Ferreira, F. F. & Marsili, M. Multi-asset minority games. *Quant. Financ.* **8,** 225–231 (2008).
37. Xie, Y.-B., Wang, B.-H., Hu, C.-K. & Zhou, T. Global optimization of minority game by intelligent agents. *Europ. Phys. J. B* **47,** 587–593 (2005).
38. Zhong, L.-X., Zheng, D.-F., Zheng, B. & Hui, P. M. Effects of contrarians in the minority game. *Phys. Rev. E* **72,** 026134 (2005).
39. Moelbert, S. & De Los Rios, P. The local minority game. *Physica A* **303,** 217–225 (2002).
40. Chen, Q., Huang, Z.-G., Wang, Y. & Lai, Y.-C. Multiagent model and mean field theory of complex auction dynamics. *New J. Phys.* **17,** 093003 (2015).
41. Moro, E. *Advances in Condensed Matter and Statistical Physics*, chap. The Minority Games: An Introductory Guide (Nova Science Publishers, 2004).
42. Yeung, C. H. & Zhang, Y.-C. Minority games. In Meyers, R. A. (ed.) *Encyclopedia of Complexity and Systems Science*, 5588–5604 (Springer New York, 2009).
43. Dyer, J. R. *et al.* Consensus decision making in human crowds. *Anim. Behav.* **75,** 461–470 (2008).
44. Wang, X. F. & Chen, G. Pinning control of scale-free dynamical networks. *Physica A* **310,** 521–531 (2002).
45. Li, X., Wang, X. & Chen, G. Pinning a complex dynamical network to its equilibrium. *IEEE Trans. Circ. Sys.* **51,** 2074–2087 (2004).
46. Chen, T., Liu, X. & Lu, W. Pinning complex networks by a single controller. *IEEE Trans. Circ. Sys.* **54,** 1317–1326 (2007).
47. Xiang, L., Liu, Z., Chen, Z., Chen, F. & Yuan, Z. Pinning control of complex dynamical networks with general topology. *Physica A* **379,** 298–306 (2007).
48. Tang, Y., Wang, Z. & Fang, J.-a. Pinning control of fractional-order weighted complex networks. *Chaos* **19,** 013112 (2009).
49. Porfiri, M. & Fiorilli, F. Node-to-node pinning control of complex networks. *Chaos* **19,** 013122 (2009).
50. Yu, W., Chen, G. & Lü, J. On pinning synchronization of complex dynamical networks. *Automatica* **45,** 429–435 (2009).
51. Albert, R., Jeong, H. & Barabási, A.-L. Error and attack tolerance of complex networks. *Nature* **406,** 378–382 (2000).

52. Callaway, D. S., Newman, M. E., Strogatz, S. H. & Watts, D. J. Network robustness and fragility: Percolation on random graphs. *Phys. Rev. Lett.* **85,** 5468 (2000).
53. Cohen, R., Erez, K., Ben-Avraham, D. & Havlin, S. Breakdown of the internet under intentional attack. *Phys. Rev. Lett.* **86,** 3682 (2001).
54. Barabási, A.-L. & Albert, R. Emergence of scaling in random networks. *Science* **286,** 509–512 (1999).
55. Catanzaro, M., Boguñá, M. & Pastor-Satorras, R. Generation of uncorrelated random scale-free networks. *Phys. Rev. E* **71,** 027103 (2005).
56. de Menezes, M. & Barabási, A. L. Fluctuations in network dynamics. *Phys. Rev. Lett.* **92,** 028701 (2004).
57. Duch, J. & Arenas, A. Scaling of fluctuations in traffic on complex networks. *Phys. Rev. Lett.* **96,** 218702 (2006).
58. Yoon, S., Yook, S.-H. & Kim, Y. Scaling property of flux fluctuations from random walks. *Phys. Rev. E* **76,** 056104 (2007).
59. Meloni, S., Gómez-Gardees, J., Latora, V. & Moreno, Y. Scaling breakdown in flow fluctuations on complex networks. *Phys. Rev. Lett.* **100,** 208701 (2008).
60. Zhou, Z., Huang, Z.-G., Yang, L., Xue, D.-S. & Wang, Y.-H. The effect of human rhythm on packet delivery. *J. Stat. Mech. Theory E.* **2010,** P08001 (2010).
61. Zhou, Z. *et al.* Universality of flux-fluctuation law in complex dynamical systems. *Phys. Rev. E* **87,** 012808 (2013).
62. Huang, Z.-G., Dong, J.-Q., Huang, L. & Lai, Y.-C. Universal flux-fluctuation law in small systems. *Sci. Rep.* **4,** 6787 (2014).
63. Ho, K., Chow, F. & Chau, H. Wealth inequality in the minority game. *Phys. Rev. E* **70,** 066110 (2004).
64. Szolnoki, A., Wang, Z. & Perc, M. Wisdom of groups promotes cooperation in evolutionary social dilemmas. *Sci. Rep.* **2,** 576 (2012).
65. Szolnoki, A. & Perc, M. Conformity enhances network reciprocity in evolutionary social dilemmas. *J. R. Soc. Interface.* **12,** 20141299 (2015).
66. Wang, T., Huang, K., Cheng, Y. & Zheng, X. Understanding herding based on a co-evolutionary model for strategy and game structure. *Chaos. Soliton. Fract.* **75,** 84–90 (2015).
67. Wu, Z.-X. & Zhang, H.-F. Peer pressure is a double-edged sword in vaccination dynamics. *Europhys. Lett.* **104,** 10002 (2013).

Acknowledgements

We thank Prof. L. Huang for helpful discussions. This work was supported by ARO under Grant W911NF-14-1-0504, and the NSF of China under Grants Nos. 11575072, 11135001 and 11275003.

Author Contributions

Z.G.H. and Y.C.L. devised the research project. J.Q.Z., Z.G.H. and R.S. performed numerical simulations. J.Q.Z., Z.G.H. and Z.X.W. analyzed the results. J.Q.Z., Z.G.H. and Y.C.L. wrote the paper.

Additional Information

Competing financial interests: The authors declare no competing financial interests.

How to cite this article: Zhang, J.-Q. *et al.* Controlling herding in minority game systems. *Sci. Rep.* **6**, 20925; doi: 10.1038/srep20925 (2016).